Cell Density-Dependent Suppression of Perlecan and Biglycan Expression by Gold Nanocluster in Vascular Endothelial Cells

Takato Hara , Misato Saeki , Misaki Shirai , Yuichi Negishi , Chika Yamamoto * , Toshiyuki Kaji *

Posted Date: 18 December 2025

doi: 10.20944/preprints202512.1621.v1

Keywords: gold-nanocluster; proteoglycan; Arf6; vascular endothelial cell

Article

Cell Density-Dependent Suppression of Perlecan and Biglycan Expression by Gold Nanocluster in Vascular Endothelial Cells

Takato Hara [1,†], Misato Saeki [1,2,†], Misaki Shirai [1,3], Yuichi Negishi [4], Chika Yamamoto [1,*] and Toshiyuki Kaji [2,*]

[1] Faculty of Pharmaceutical Sciences, Toho University, 2-2-1 Miyama, Funabashi, Chiba 274-8510, Japan
[2] Faculty of Pharmaceutical Sciences, Tokyo University of Science, 6-3-1 Niijuku, Katsushika-ku, Tokyo 125-8585, Japan
[3] Research fellow of the Japanese society for the promotion of science, 5-3-1 Kojimachi, Chiyoda, Tokyo 102-0083, Japan
[4] Institute of Multidisciplinary Research for Advanced Materials, Tohoku University, 2-1-1 Katahira, Aoba-ku, Sendai 980-8577, Japan
* Correspondence: yamamoto@phar.toho-u.ac.jp (C.Y.); t-kaji@rs.tus.ac.jp (T.K.)
† Those who contributed equally.

Highlights

What are the main findings?

- $Au_{25}(SG)_{18}$, a nanoscale gold cluster with low electrophilicity, accumulates in vascular endothelial cells at low cell density and suppresses perlecan expression by inactivating ADP-ribosylation factor 6 (Arf6).
- $Au_{25}(SG)_{18}$ also decreases biglycan expression in vascular endothelial cells at low cell density; however, the underlying mechanisms remain unclear.

What are the implications of the main findings?

- This study suggests that organic–inorganic hybrid molecules modulate Arf6-mediated protein transport to the extracellular space, revealing a novel mechanism for proteoglycan synthesis regulation.
- Arf6-mediated extracellular transport plays a critical role in maintaining vascular homeostasis, serving as a potential target to modulate endothelial function and vascular diseases.

Abstract

Proteoglycans are macromolecules consisting of a core protein and one or more glycosaminoglycan side chains. Proteoglycans synthesized by vascular endothelial cells modulate various functions, such as anticoagulant activity and vascular permeability. We previously reported that some heavy metals interfere with proteoglycan expression and that organic–inorganic hybrid molecules, such as metal complexes and organometallic compounds, serve as useful tools to analyze proteoglycan synthesis mechanisms. However, the effects of metal compounds lacking electrophilicity on proteoglycan synthesis remain unclear. $Au_{25}(SG)_{18}$, a nanoscale gold cluster consisting of a metal core protected by gold–glutathione complexes, exhibits extremely low intramolecular polarity. In this study, we investigated the effect of $Au_{25}(SG)_{18}$ on proteoglycan synthesis in vascular endothelial cells. $Au_{25}(SG)_{18}$ accumulated significantly in vascular endothelial cells at low cell density and suppressed the expression of perlecan, a major heparan sulfate proteoglycan in cells, by inactivating ADP-ribosylation factor 6 (Arf6). Additionally, $Au_{25}(SG)_{18}$ reduced the expression of biglycan, a small dermatan sulfate proteoglycan, in vascular endothelial cells at low cell density; however, the underlying mechanisms remain unclear. Overall, our findings suggest that organic–inorganic hybrid molecules regulate the activity of Arf6-mediated protein transport to the extracellular space and that

 doi:10.20944/preprints202512.1621.v1

perlecan is regulated through this mechanism, highlighting the importance of Arf6-mediated extracellular transport for maintaining vascular homeostasis.

Keywords: gold-nanocluster; proteoglycan; Arf6; vascular endothelial cell

1. Introduction

Vascular endothelial cells covering the lumen of blood vessels in a monolayer function as a barrier between the blood and subendothelial matrix to allow specific plasma components to penetrate tissues [1]. The endothelial monolayer also regulates the blood coagulation–fibrinolytic system by secreting the procoagulant tissue factor [2], prostacyclin [3], which inhibits platelet aggregation, anticoagulant thrombomodulin [4], and fibrinolytic tissue plasminogen activator [5] and its inhibitor (plasminogen activator inhibitor-1) [6]. Proteoglycans (PGs) are among the anticoagulant molecules found in vascular endothelial cell layers. They are macromolecules consisting of glycosaminoglycan (GAG) chains covalently bound to a core protein backbone. They are ubiquitously present in the extracellular matrix and cell membranes of animal tissues [7]. PG molecules are classified based on the type of GAG chain attached to their core protein. Vascular endothelial cells predominantly synthesize two types of PGs: Heparan sulfate PGs (HSPGs) and dermatan sulfate PGs (DSPGs) [8]. HSPGs include perlecan, a large molecular species constituting the basement membrane [9], and transmembrane syndecan-1 and syndecan-4 [10]. Biglycan is the primary DSPG secreted into the extracellular space [11]. Endothelial PGs synthesized by vascular endothelial cells contribute to the anticoagulant properties of the vascular endothelium [12,13]. Specifically, heparan sulfate chains of perlecan and syndecan family bind to and activate antithrombin III to inhibit thrombin, which converts fibrinogen into fibrin [14]. Meanwhile, dermatan sulfate chains of biglycan activate heparin cofactor II, thereby inhibiting thrombin [15]. Considering the important role of PGs in maintaining the anticoagulant properties of vascular endothelial cells, their synthesis mechanisms in cells warrant further investigation.

Endothelial PG synthesis is regulated by various growth factors/cytokines, including transforming growth factor (TGF)-β_1 [16,17], fibroblast growth factor (FGF)-2 [18], connective tissue growth factor [19], vascular endothelial growth factor-165 [20], tumor necrosis factor-α [21], and interleukin-1β [22]. The types of PGs are regulated by growth factors/cytokines and vary depending on the specific growth factors/cytokines. For example, TGF-β_1 induces the synthesis of both perlecan and biglycan at high cell density and only that of biglycan at low cell density. Vascular endothelial growth factor-165 selectively induces perlecan synthesis [20]. Connective tissue growth factor suppresses biglycan synthesis but induces decorin synthesis in the cells at low cell density [19]. Additionally, FGF-2 induces syndecan-4 synthesis via different molecular mechanisms depending on the cell density [23]. These reports suggest that the expression of endothelial PG species is differentially regulated depending on both the types of growth factors/cytokines and cell density.

We previously studied the alteration in PG synthesis by some heavy metals in vascular endothelial cells. Perlecan synthesis was found to be induced by cadmium [24]. In contrast, lead suppressed perlecan synthesis in vascular endothelial cells [25]. This suppression by lead was mediated by the epidermal growth factor receptor–extracellular signal-regulated kinase (ERK)-1/2–cyclooxygenase-2–PGI_2 pathway [26] and inhibited the proliferation of vascular endothelial cells by decreasing the availability of endogenous FGF-2 [27]. These results suggest that some cationic heavy metals influence endothelial PG synthesis. Therefore, we investigated whether organic–inorganic hybrid molecules affect PG synthesis in endothelial cells. Copper (II) bis(diethyldithiocarbamate) induced syndecan-4 synthesis via activation of p38 mitogen-activated protein kinase (MAPK) in vascular endothelial cells [28]. Syndecan-4 synthesis was also induced by organic–inorganic hybrid molecules with a 1,10-phenanthroline structure activation of the hypoxia-inducible factor-1α/β pathway via inhibition of prolyl hydroxylase-domain-containing protein 2 [29]. Additionally, dichloro(2,9-dimethyl-1,10-phenanthroline)zinc(II) modulated endothelial perlecan synthesis

 doi:10.20944/preprints202512.1621.v1

depending on the cell density [30]. *Sb*-Phenyl-*N*-methyl-5,6,7,12-tetrahydrodibenz[*c,f*][1,5]azastibocine also induced perlecan synthesis in vascular endothelial cells at high cell density [31]. All inorganic metals and organometallic compounds that we have identified to date possess electrophilic properties. However, whether the expression of PG molecular species is regulated by non-electrophilic compounds remains unclear.

Recently, nanotechnology has made remarkable progress, showing potential to solve societal issues in various fields, such as materials, energy, environment, information communication, and healthcare. Consequently, development of stable and highly functional metal nanoclusters consisting of several hundred metal atoms within 1–2 nm has also made considerable progress. Particularly, gold nanoclusters exhibit high-functioning properties unique to their size that are not observed in metals other than gold, such as catalytic activity [32,33], optical activity [34], and luminescent [35,36], and magnetic [37,38] properties. These nanomaterials have attracted significant attention in various fields, such as fuel cells, photocatalysts, and solar cells. Thiolate-protected gold clusters ($Au_n(SR)_m$) exhibit a structure in which a gold–thiolate complex (-SR-Au-SR-) is bound to the surface of the gold core, and Au-Au and Au-SR bonds form a rigid cyclic network, providing high stability [39]. Particularly stable clusters composed of gold atoms with magic numbers (n = 25, 38, 102, and 144) have been identified [40,41]. Glutathione-protected $Au_{25}(SG)_{18}$ exhibits a diameter of approximately 1 nm [42], and its gold core, which consists of 13 gold atoms in an icosahedral structure, exhibits minimal polarity within the molecule [43]. These reports suggest that $Au_{25}(SG)_{18}$ is a non-electrophilic metal compound. In this study, we aimed to determine the effect of this gold cluster $Au_{25}(SG)_{18}$ on PG synthesis in vascular endothelial cells.

2. Materials and Methods

2.1. Materials

Bovine aortic endothelial cells were obtained from Cell Applications (San Diego, CA, USA). Tissue culture dishes and plates were purchased from AGC Techno Glass (Shizuoka, Japan). Dulbecco's modified Eagle's medium (DMEM) and Ca^{2+}- and Mg^{2+}-free phosphate-buffered saline were obtained from Nissui Pharmaceutical (Tokyo, Japan). $Au_{25}(SG)_{18}$ was synthesized as previously described [44]. Standard gold nanoparticles (AuNPs; 5 nm) were purchased from Cytodiagnostics (Burlington, Canada). Universal negative control small interfering RNA (siRNA), GeneAce SYBR qPCR Mix α, and ISOGEN II were purchased from NipponGene (Tokyo, Japan). Sulfur-35 ($[^{35}S]Na_2SO_4$; NEX041H) and Insta-Gel Plus were obtained from PerkinElmer (Waltham, MA, USA). GGA3-PBD Agarose Beads were purchased from Cell Biolabs (San Diego, CA, USA), and Chondroitinase ABC was obtained from Sigma-Aldrich (St. Louis, MO, USA). Fetal bovine serum, Lipofectamine RNAiMAX, high-capacity cDNA reverse transcription kit, MagicMark XP Western Protein Standard, and bicinchoninic acid (BCA) protein assay kit were purchased from Thermo Fisher Scientific (Waltham, MA, USA). Amersham Hybond P 0.2-μm polyvinylidene difluoride and diethylaminoethyl-Sephacel were obtained from GE Healthcare (Chicago, IL, USA). Heparinase II and III were purchased from IBEX Pharmaceuticals (Quebec, Canada). Anti-biglycan (ab94460) and anti-ARF6 (EPR8357; ab131261) antibodies were obtained from Abcam (Cambridge, UK). Anti-glyceraldehyde-3-phosphate dehydrogenase antibody was purchased from Wako Pure Chemical Industries (Osaka, Japan). Anti-perlecan antibody (E-6; sc-377219) was obtained from Santa Cruz Biotechnology (Santa Cruz, CA, USA). Anti-rabbit (#7074) and anti-mouse (#7076) secondary antibodies were purchased from Cell Signaling Technology (Danvers, MA, USA). Chemi-Lumi One Super and other reagents of the highest grade available were obtained from Nacalai Tesque (Kyoto, Japan).

2.2. Cell Culture and siRNA Transfection

Vascular endothelial cells were cultured in DMEM supplemented with 10% fetal bovine serum at 37 °C in a humidified atmosphere of 5% CO_2 until confluence. Subsequently, the cells were

 doi:10.20944/preprints202512.1621.v1

transferred to 100-mm dishes and 24-well plates at a density of 1×10^4 cells/cm^2 and cultured for 24 h (sparse culture) or 35- and 60-mm dishes and 24-well plates until confluence (dense culture). In another experiment, the cells were cultured in DMEM supplemented with 10% fetal bovine serum at 37 °C in a humidified atmosphere of 5% CO_2 until 80–90% confluence. Next, siRNA was transfected into the cells using Lipofectamine RNAiMAX, as previously described [17]. The final concentrations of siRNA and Lipofectamine RNAiMAX were 30 nM and 0.15%, respectively. The following sequences of siRNA sense and antisense strands were used: Bovine *Arf6* siRNA, 5′-CGGTCATTGATAATGCGGdTdT-3′ (sense) and 5′-GCACCGCAUUAUCAAUGACdTdT-3′ (antisense). After 24 h of incubation, the transfected cells were transferred to 60-mm dishes at densities of 1 and 6×10^4 cells/cm^2, cultured for 24 h, and used for subsequent experiments.

2.3. Incorporation of [^{35}S]Sulfate into GAGs

Dense and sparse cultures of vascular endothelial cells were seeded in 24-well plates. After washing twice with serum-free DMEM, the cells were treated with various concentrations of $Au_{25}(SG)_{18}$ (0.05, 0.10, 0.20, 0.39, and 0.78 μg/mL) in fresh serum-free DMEM and incubated in the presence of [^{35}S]sulfate (1 MBq/mL) for 24 h. Subsequently, [^{35}S]sulfate incorporation into GAGs was determined via cetylpyridinium chloride precipitation, as previously described [16].

2.4. Quantitative Reverse Transcription-Polymerase Chain Reaction (qRT-PCR)

Dense and sparse cultures of vascular endothelial cells cultured in 35- and 100-mm dishes, respectively, were treated with various concentrations of $Au_{25}(SG)_{18}$ (0.05, 0.1, 0.2, 0.39, 0.78, 3.13, and 12.5 μg/mL) for 2, 4, 8, 12, and 24 h. Then, total RNA was extracted from the cells and reverse-transcribed into cDNA as previously described [45]. RT-PCR was performed on the CFX Connect real-time PCR system (BioRad) using the GeneAce SYBR qPCR mix α with 5 ng of cDNA and 0.2 μM of the following primers: Bovine perlecan, 5′-ATGGCAGCGATGAAGCGGAC-3′ (forward) and 5′-TTGTGGACACGCAGCGGAAC-3′ (reverse); bovine biglycan, 5′-GCTGCCACTGCCATCTGAG-3′ (forward) and 5′-CGAGGACCAAGGCGTAG-3′ (reverse); bovine syndecan-1, 5′-GGGGACGACAGTGACAACTTCTC-3′ (forward) and 5′-CCTCCTTCTGGGCGGTGA-3′ (reverse); bovine syndecan-4, 5′-TTGCCGTCTTCCTCGTGC-3′ (forward) and 5′-AGGCGTAGAACTCATTGGTGG-3′ (reverse); bovine beta-2-microglobulin (*B2M*), 5′-CCATCCAGCGTCCTCCAAAGA-3′ (forward) and 5′-TTCAATCTGGGGTGGATGGAA-3′ (reverse). The mRNA levels of perlecan, biglycan, syndecan-1, syndecan-4, and *B2M* were quantified using the relative standard curve method. The fold change in target gene intensity was normalized to B2M intensity.

2.5. PG Core Protein Expression and Western Blotting Analysis

Sparse vascular endothelial cells were prepared in 100-mm dishes. The cells were washed twice with serum-free DMEM and treated with 0.20 and 0.78 μg/mL $Au_{25}(SG)_{18}$ in fresh serum-free DMEM for 24 h. PGs accumulated in the cell layer were extracted from the whole cell lysate, and the conditioned medium of vascular endothelial cells was concentrated as previously described [17]. Concentrated PGs were digested with heparinase II/III in 100 mM Tris-HCl (pH 7.0) containing 10 mM calcium acetate and 18 mM sodium acetate (for perlecan core protein) or chondroitinase ABC in 50 mM Tris-HCl (pH 8.0) containing 1 mg/mL bovine serum albumin and 3 mM sodium acetate (for perlecan core protein). After digesting the heparan and chondroitin/dermatan sulfate chains with heparinase II/III and chondroitinase ABC, respectively, PG core protein bands were detected via western blotting analysis, and the molecular mass of the PG core protein was determined via sodium dodecyl sulfate-polyacrylamide gel electrophoresis. Western blotting analysis was performed on samples obtained from multiple independent experiments at least twice to confirm reproducibility.

 doi:10.20944/preprints202512.1621.v1

2.6. Intracellular Accumulation of Gold Atoms

Vascular endothelial cells transfected siRNA were treated with 0.78 μg/mL of $Au_{25}(SG)_{18}$. After a 24-h incubation, the cell layer was harvested with 80 μL of 50 mM Tris-HCl buffer solution (pH 6.8) containing 2% sodium dodecyl sulfate and 10% glycerol. The samples were incubated as previously described [46] and dissolved in 5 mL of 0.1 M HNO_3. The gold atom content was analyzed via inductively coupled plasma mass spectrometry (Nexion 300S; PerkinElmer) under conditions optimized for a plasma output of 1600 W, plasma gas flow of 18.0 L/min, and nebulizer gas flow rate of 0.94 L/min. Another portion of the cell lysate was analyzed for protein content using the BCA protein assay kit to express gold content as pmol/mg protein.

2.7. Arf6 Activation (GTP-Bound Arf6 Pulldown) Assay

Sparse cultures of vascular endothelial cells grown in 100-mm dishes were treated with 0.2 and 0.78 μg/mL $Au_{25}(SG)_{18}$ for 12 h. After incubation, the cells were washed twice with and Ca^{2+}- and Mg^{2+}-free phosphate-buffered saline and lysed with 100 μL of assay/lysis buffer (25 mM HEPES [pH7.5], 150 mM NaCl, 10 mM $MgCl_2$, 1 mM EDTA, 2% glycerol, and 1% NP-40). The lysates were centrifuged at 14,000 × *g* for 10 min at 4 °C. Protein concentrations in the collected supernatants were determined using the BCA protein assay kit. The samples were diluted to 400 μg protein in 1 mL with the assay/lysis buffer. The negative control sample was prepared according to the protocol of the Arf6 Activation Assay Kit (STA-407-6; Cell Biolabs). To each sample, 40 μL of GGA3-PBD Agarose Bead solution was added and rotated at 4 °C for 1 h. Then, the samples were centrifuged at 14,000 × *g* for 3 min at 4 °C, and the supernatants were discarded. The precipitated beads were washed with 500 μL of the assay/lysis buffer. The washing step was repeated thrice. After the final wash, 20 μL of loading buffer (50 mM Tris [pH 6.8], 8% glycerol, 2% sodium dodecyl sulfate, 5% 2-mercaptoethanol, and 0.002% bromophenol blue) was added to each sample. The samples were boiled at 95 °C for 5 min. Finally, GTP-bound Arf6 protein expression was measured via western blotting analysis, as described above.

2.8. Statistical Analyses

The data were statistically analyzed via analysis of variance, followed by Bonferroni's multiple *t*-test when applicable, using the Statcel4 software (OMS, Tokyo, Japan). Statistical significance was set at $P < 0.05$.

3. Results

3.1. $Au_{25}(SG)_{18}$ Suppresses PG Synthesis in Sparse Cultures of Vascular Endothelial Cells

First, we investigated the effects of $Au_{25}(SG)_{18}$ and AuNPs on [^{35}S]sulfate incorporation into the PGs synthesized by vascular endothelial cells. $Au_{25}(SG)_{18}$ did not modulate [^{35}S]sulfate-labeled PG accumulation in the cell layer and conditioned medium of the dense cultures of vascular endothelial cells (Figure 1A). In contrast, in sparse cultures, $Au_{25}(SG)_{18}$ decreased [^{35}S]sulfate-labeled PG accumulation in both the cell layer and conditioned medium in a concentration-dependent manner (Figure 1B). Notably, AuNPs did not affect PG synthesis in dense cultures (Figure 1C); however, they exerted similar but weaker effects than $Au_{25}(SG)_{18}$ in sparse cultures (Figure 1D).

 doi:10.20944/preprints202512.1621.v1

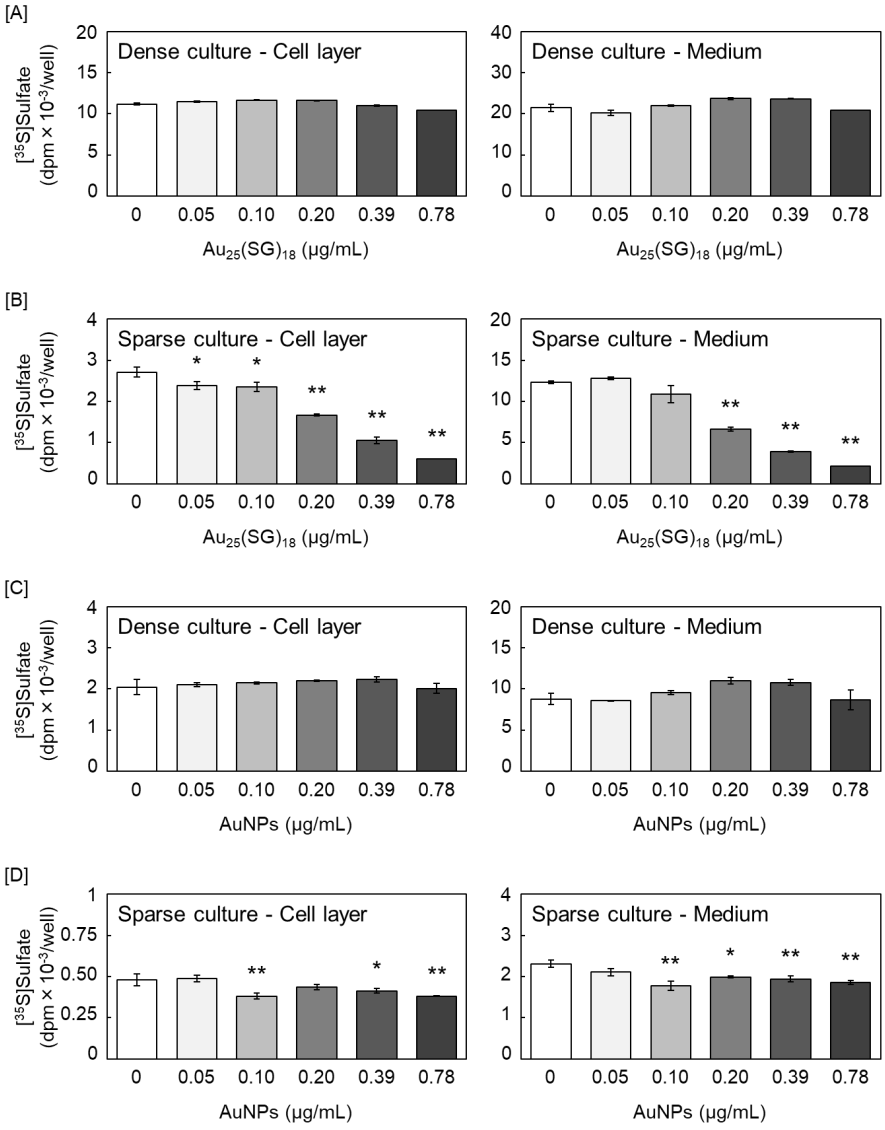

Figure 1. [^{35}S]Sulfate incorporation into glycosaminoglycans (GAGs) accumulated in the cell layer (left panels) and conditioned medium (right panels). Vascular endothelial cells in [A and C] dense and [B and D] sparse cultures treated with [A and B] $Au_{25}(SG)_{18}$ and [C and D] gold nanoparticles (AuNPs; 0.05, 0.1, 0.2, 0.39, and 0.78 μg/mL) for 24 h. Values are expressed as the mean ± standard error (S.E.) of four samples. *$P < 0.05$ and **$P < 0.01$ vs. the corresponding control.

3.2. Perlecan and Biglycan Expression Is Suppressed by $Au_{25}(SG)_{18}$ in Sparse Cultures of Vascular Endothelial Cells

Based on these results, we further explored the type(s) of PGs synthesized by vascular endothelial cells that were modulated by $Au_{25}(SG)_{18}$. In dense cultures, $Au_{25}(SG)_{18}$ showed no concentration- and time-dependent changes in any PG type (Figure 2A). In contrast, perlecan and biglycan mRNA expression levels were dose- and time-dependently decreased by $Au_{25}(SG)_{18}$ in sparse cultures (Figure 2B). Additionally, core protein expression levels of perlecan and biglycan were dose-dependently decreased by $Au_{25}(SG)_{18}$ in the cell layer and conditioned medium, respectively, in sparse cultures (Figure 3).

 doi:10.20944/preprints202512.1621.v1

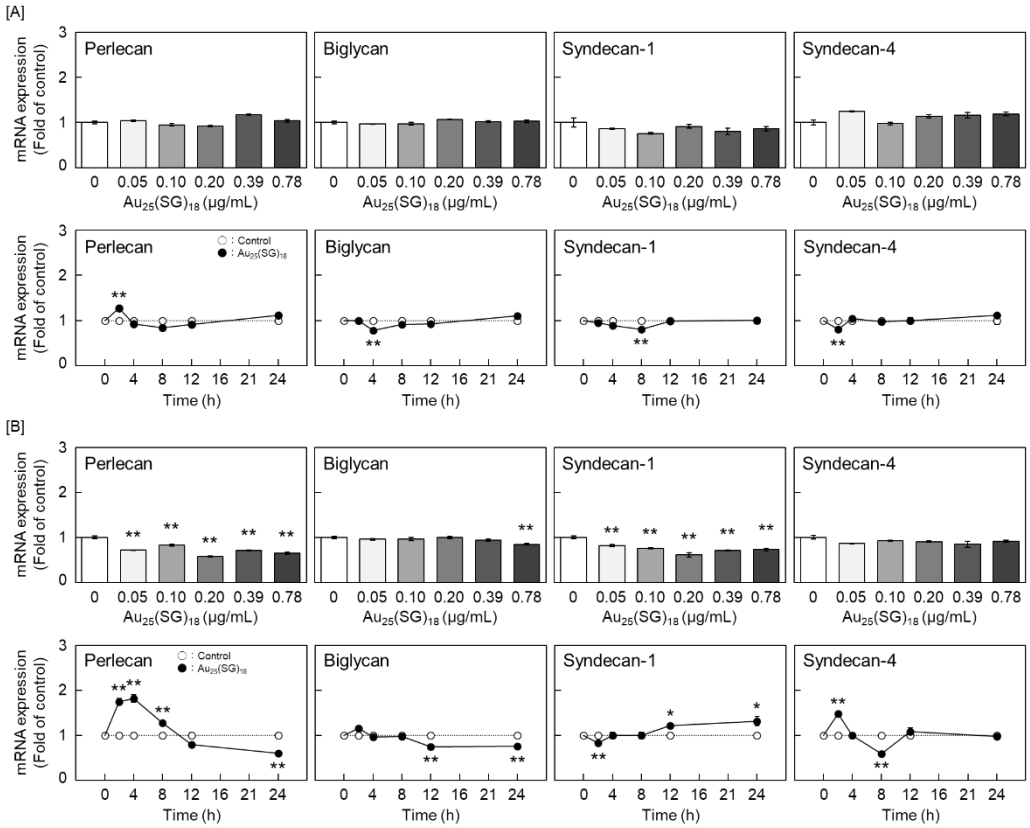

Figure 2. Perlecan, biglycan, syndecan-1, and syndecan-4 mRNA levels in vascular endothelial cells after treatment with $Au_{25}(SG)_{18}$. [A] Dense and [B] sparse cultures of bovine aortic endothelial cells incubated for 12 h in the absence or presence of $Au_{25}(SG)_{18}$ (0.05, 0.1, 0.2, 0.39, and 0.78 μg/mL; upper panels) or 2, 4, 8, 12, and 24 h in the absence or presence of $Au_{25}(SG)_{18}$ (0.2 μg/mL; lower panels). Values are expressed as the mean ± S.E. of four samples. *$P < 0.05$ and **$P < 0.01$ vs. the corresponding control.

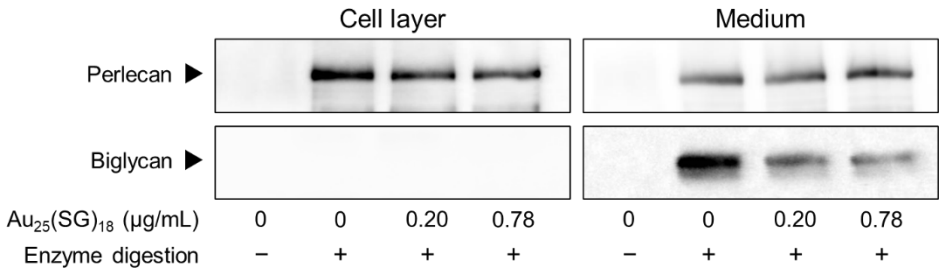

Figure 3. Perlecan and biglycan core protein levels in vascular endothelial cells after treatment with $Au_{25}(SG)_{18}$. Sparse cultures of bovine aortic endothelial cells were incubated for 24 h in the absence or presence of $Au_{25}(SG)_{18}$ (0.2 and 0.78 μg/mL).

3.3. $Au_{25}(SG)_{18}$ Does Not Affect the mRNA Expression Levels of Perlecan and Biglycan in Dense Cultures of Vascular Endothelial Cells, Even at High Concentrations

We previously reported that $Au_{25}(SG)_{18}$ is less likely to accumulate in vascular endothelial cells at high cell density [46]. To determine whether this is why the expression levels of perlecan and biglycan were not reduced by $Au_{25}(SG)_{18}$ in our dense cultures, we examined the effects of high concentrations of $Au_{25}(SG)_{18}$ on the mRNA levels of these PGs. Notably, perlecan and biglycan levels were not affected by high concentrations of $Au_{25}(SG)_{18}$ (Figure 4).

 doi:10.20944/preprints202512.1621.v1

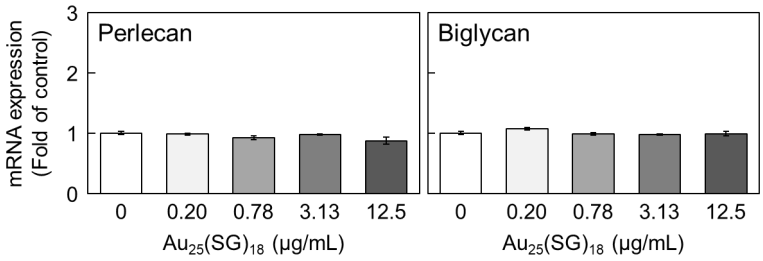

Figure 4. Perlecan and biglycan mRNA levels in dense cultures of vascular endothelial cells after treatment with $Au_{25}(SG)_{18}$. Dense cultures of bovine endothelial cells were incubated for 12 h in the absence or presence of $Au_{25}(SG)_{18}$ (0.2, 0.78, 3.13, and 12.5 μg/mL). Values are expressed as the mean ± S.E. of four samples.

3.4. Role of Arf6 in the Regulation of Cell Density-Dependent PG Synthesis

Because $Au_{25}(SG)_{18}$ regulated PG synthesis in a cell density-dependent manner, we focused on Arf6, a member of the Ras superfamily that includes small GTPases [47] and a GTP-binding multifunctional molecule activated at low cell density [48]. As Arf6 is involved in endocytosis, we examined whether Arf6 participates in the cell density-dependent cellular uptake of $Au_{25}(SG)_{18}$. We confirmed that Arf6 expression was suppressed by siRNA transfection (Figure 5A) and compared intracellular gold accumulation between the Arf6-suppressed and control groups at low and high cell densities. Notably, no significant difference in gold accumulation was observed between the two groups, with no involvement of Arf6 in the cellular uptake of $Au_{25}(SG)_{18}$ (Figure 5B). Next, we examined whether Arf6 contributes to the suppression of perlecan and biglycan expression by $Au_{25}(SG)_{18}$ in sparse cultures. The mRNA levels of perlecan and biglycan were reduced by *Arf6* knockdown in the absence of $Au_{25}(SG)_{18}$. Perlecan suppression by $Au_{25}(SG)_{18}$ was maintained upon control siRNA transfection but abolished at the mRNA and core protein levels following *Arf6* knockdown. In contrast, biglycan mRNA and core protein expression was not suppressed upon siRNA transfection. The mechanism by which Arf6 affected biglycan expression could not be determined in this experimental system (Figure 5C and D). Specifically, in vascular endothelial cells treated with *Arf6* siRNA, no reduction in biglycan mRNA levels was observed following $Au_{25}(SG)_{18}$ treatment. Although the exact mechanism remains unclear, this phenomenon was confirmed in several experiments. In the steady state, Arf6 exists in an inactive form bound to GDP. When the cell receives stimuli such as growth factors or hormones, GDP dissociates from Arf6, and GTP binds to the site instead. Here, treatment with $Au_{25}(SG)_{18}$ suppressed GTP-bound Arf6 expression in endothelial cells in sparse cultures, without affecting total Arf6 expression (Figure 6). These results suggest that $Au_{25}(SG)_{18}$ reduces Arf6 activity in vascular endothelial cells at low cell density and suppresses perlecan expression by modulating downstream signaling.

 doi:10.20944/preprints202512.1621.v1

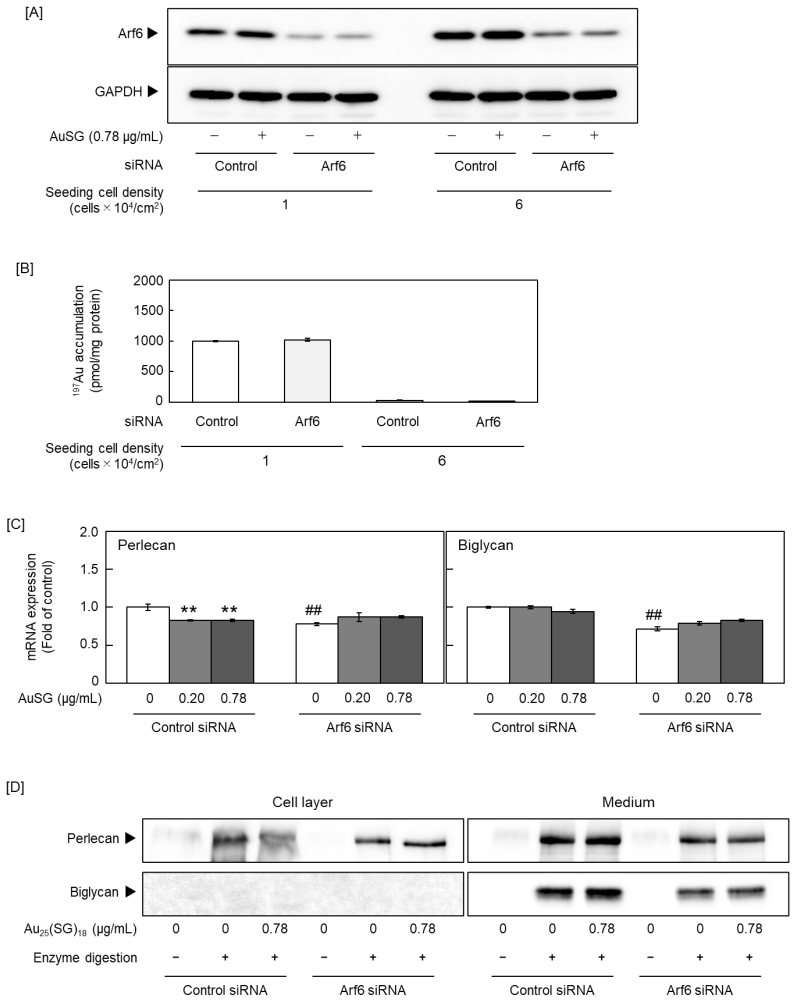

Figure 5. Effect of ADP-ribosylation factor 6 (Arf6) on the cell density-dependent suppression of proteoglycan (PG) synthesis by $Au_{25}(SG)_{18}$ in sparse vascular endothelial cells. [A] Arf6 protein expression and [B] intracellular accumulation of $Au_{25}(SG)_{18}$. Bovine aortic endothelial cells transfected with the negative control or Arf6 small interfering RNA (siRNA) were seeded at 1 and 6 × 10^4 cells/cm^2, cultured for 24 h, and treated with $Au_{25}(SG)_{18}$ (0.78 μg/mL each) for 24 h. Values are expressed as the mean ± S.E. of three samples. The [C] mRNA and [D] core protein levels of perlecan and biglycan. Bovine aortic endothelial cells transfected with the negative control or Arf6 siRNA were seeded at 1 × 10^4 cells/cm^2, cultured for 24 h, and treated with $Au_{25}(SG)_{18}$ (0.2 and 0.78 μg/mL) for 24 h. Values are expressed as the mean ± S.E. of four samples. $^{**}P < 0.01$ vs. without $Au_{25}(SG)_{18}$; $^{\#\#}P < 0.01$ vs. siControl.

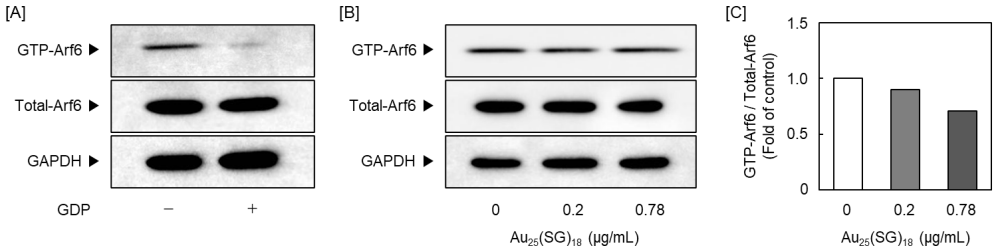

Figure 6. Arf6 activation in sparse cultures of vascular endothelial cells. Activated-Arf6 (GTP-Arf6) levels were measured via GGA3 pull-down and western blotting assays. [A] Confirmation of the experimental system. Sparse cultures of vascular endothelial cells were harvested after incubation for 12 h. Negative control samples were reacted with GDP before pull-down assay. [B] Sparse cultures of vascular endothelial cells were incubated for 12 h in the absence or presence of $Au_{25}(SG)_{18}$ (0.2 and 0.78 μg/mL). [C] Ratio of the intensity of GTP-Arf6 in [B] to that of Total-Arf6.

 doi:10.20944/preprints202512.1621.v1

4. Discussion

PGs are biomolecules that play a crucial role in maintaining blood vessel homeostasis. Disruption of vascular homeostasis is closely associated with the initiation and progression of various diseases and conditions, such as cancer, stroke, and heart disease. Therefore, understanding PG synthesis mechanisms in endothelial cells, which regulate vascular functions, is important for vascular homeostasis. Although many studies have investigated the functions of PG species and their involvement in pathological conditions, only a few have focused on the mechanisms regulating their expression. In this study, we analyzed the regulatory mechanisms of PG synthesis in vascular endothelial cells using $Au_{25}(SG)_{18}$, which possesses no electrophilic properties. We found that: (1) Similar to AuNPs, $Au_{25}(SG)_{18}$ did not show cytotoxicity in endothelial cells, regardless of cell density, (2) despite not being electrophilic, $Au_{25}(SG)_{18}$ accumulated in cells similarly to AuNPs, with higher uptake observed at low density, (3) $Au_{25}(SG)_{18}$ significantly suppressed perlecan and biglycan synthesis more potently than AuNPs, (4) $Au_{25}(SG)_{18}$ suppressed perlecan and biglycan expression only in endothelial cells at low cell density, (5) $Au_{25}(SG)_{18}$ suppressed perlecan expression via Arf6, and (6) Arf6 was involved in the induction of perlecan expression in endothelial cells at low cell density. Collectively, these results suggest that $Au_{25}(SG)_{18}$ negatively modulates perlecan and biglycan synthesis in vascular endothelial cells at low cell density, without causing cytotoxicity. Notably, $Au_{25}(SG)_{18}$, which is not an electrophilic substance, accumulated and affected PG synthesis in vascular endothelial cells at low cell density. Furthermore, these effects were not observed with AuNPs, suggesting that the negative modulation of perlecan and biglycan synthesis in vascular endothelial cells is unique to $Au_{25}(SG)_{18}$.

Gold compounds, such as gold thiolates [49] and auranofin [50], are widely used in medicine to treat rheumatoid arthritis. Recently, their applications have been extended to other areas such as biological diagnostics using nanoscale gold particles [51], drug delivery [52], bioimaging [53,54], and radiation therapy [55,56]. With the accelerated development of gold-containing NPs, research on their toxicity and in vivo distribution has also increased. Accumulation of AuNPs in cells is affected by their size, charge, and surface modifications; AuNPs larger than 50 nm cannot pass through the reticuloendothelial system barrier [57,58], whereas those smaller than 50 nm accumulate in cells [59]. Positively charged AuNPs are highly toxic [60] and induce cell death [61]. Notably, AuNP charge can be modified by their coating, with neutral AuNPs exhibiting lower cellular uptake than negatively charged AuNPs [62,63]. These results suggest that the size and charge of NPs are important for their biological activities, including cytotoxicity upon intracellular accumulation. $Au_{25}(SG)_{18}$ exhibits a diameter of approximately 1 nm [42] and low intramolecular polarity; therefore, it possibly accumulates easily in cells and exhibits low cytotoxicity. A previous study reported low cytotoxicity of $Au_{25}(SG)_{18}$ in vascular endothelial cells [46]; in this study, its intracellular accumulation was lower than that of AuNPs because of its lack of charge. Nonetheless, it markedly suppressed perlecan and biglycan expression in vascular endothelial cells in sparse cultures. These results suggest that $Au_{25}(SG)_{18}$ exhibits higher biological activity than AuNPs. Although the mechanisms underlying the biological activities of $Au_{25}(SG)_{18}$ remain unknown, it is a useful analytical tool to elucidate the regulatory mechanisms of PG synthesis in vascular endothelial cells.

Previous studies have reported that the internalization of lipoic acid-protected gold nanoclusters into cells occurs via endocytosis, which is involved in the nutrient uptake and metabolic turnover of cell surface molecules [64,65]. Clathrin and caveolae are molecules that regulate the formation of endocytic vesicles [66,67]. Based on the morphological characteristics, endocytosis is broadly classified into four types: (i) Clathrin-dependent endocytosis, (ii) caveolae-dependent endocytosis, (iii) clathrin/caveolae-independent endocytosis, and (iv) macropinocytosis, which is associated with the dynamics of the actin cytoskeleton [68]. Clathrin-mediated endocytosis is not affected during mitosis, and clathrin internalized during this process does not return to the membrane surface until late telophase [69]. In contrast, caveolae are membrane structures commonly found in endothelial cells [70]. Caveolin, a key molecule forming caveolae, actively translocates into cells during cell division and localizes to endosomal structures. It subsequently returns to the cell surface during or after cytokinesis

 doi:10.20944/preprints202512.1621.v1

[71] and regulates nutrient and receptor transport in proliferating cells [72]. These reports suggest that clathrin-mediated endocytosis is unaffected by the cell cycle, whereas caveolae-mediated endocytosis is more likely to occur during mitosis in endothelial cells. Therefore, $Au_{25}(SG)_{18}$ translocates into cells via caveolae-dependent endocytosis, which is negatively dependent on the cell density.

Synthesis of PGs, particularly syndecans and transmembrane-type small HSPGs, influences membrane trafficking and recycling [73,74]. Whether Arf6 is involved in the synthesis of perlecan, a large HSPG that exists in the extracellular matrix of vascular endothelial cells, remains unclear. However, Arf6 possibly regulates perlecan synthesis, as ARF6 has been reported regulate the synthesis of fusogenic lipids, which are involved in exocytosis, a process related to perlecan secretion [73]. In this study, $Au_{25}(SG)_{18}$ significantly suppressed perlecan synthesis in vascular endothelial cells, indicating that Arf6 plays a key role in the regulation of perlecan secretion.

Arf6 is activated by converting its bound GDP to GTP, and this exchange is triggered by guanine nucleotide exchange factors (GEFs) [75]. Arf6 returns to its inactivated state by hydrolyzing bound GTP to GDP through its own GTPase activity. Typically, GTPase activity of small G proteins, including Arf6, is very low; therefore, assistance from a GTPase-activating protein is essential for the hydrolysis of GTP bound to Arf6 into GDP [76]. Therefore, both GEFs and GTPase-activating protein are important for maintaining Arf6 function [77]. In this study, perlecan suppression by $Au_{25}(SG)_{18}$ was abolished in vascular endothelial cells, further suppressing Arf6 expression. Additionally, $Au_{25}(SG)_{18}$ reduced the amount of GTP-bound Arf6, suggesting that $Au_{25}(SG)_{18}$ negatively regulates perlecan synthesis by inhibiting the activity of Arf6 GEFs, such as the cytohesin family members [78].

We previously reported that heavy metals and organic–inorganic hybrid molecules regulate PG expression via MAPKs, which regulate cell proliferation, differentiation, and growth. Lead suppresses perlecan expression via the epidermal growth factor receptor–ERK1/2–cyclooxygenase-2–PGI_2 pathway [26] and copper complex copper(II) bis(diethyldithiocarbamate)-induced syndecan-4 expression mediated by p38 MAPK [28]. However, among the representative MAPKs (ERK1/2, JNK, and p38 MAPK), $Au_{25}(SG)_{18}$ suppressed the activation of ERK1/2 but had no effect on the activation of JNK and p38 MAPK (Figure S1). This suggests that $Au_{25}(SG)_{18}$ suppresses perlecan and biglycan expression independently of the MAPK pathway. Perlecan is a component of the basement membrane [9] and promotes the binding of FGF-2 to receptors on endothelial cells via heparan sulfate chains, thereby enhancing their proliferation and migration [79]. Arf6 stimulates epithelial cell migration [80], and its activation promotes fibroblast proliferation [81]. Although the detailed regulatory mechanisms remain unclear, these findings suggest that Arf6 regulates the proliferation and migration of endothelial cells, contributing to the maintenance of vascular homeostasis. Overall, this study revealed that $Au_{25}(SG)_{18}$ regulated perlecan expression and identified Arf6 as an important factor for this regulation in vascular endothelial cells, highlighting non-electrophilic organometallic compounds as useful tools for biological function analysis.

Supplementary Materials: The following supporting information can be downloaded at: https://www.mdpi.com/article/doi/s1, Figure S1.

Author Contributions: Conceptualization, Hara. and Kaji; methodology, Hara and Saeki; validation, Saeki; formal analysis, Hara and Saeki; investigation, Saeki; resources, Negishi and Yamamoto; data curation, Hara; writing—original draft preparation, Hara, Saeki and Shirai; writing—review and editing, Kaji; visualization, Hara and Saeki; supervision, Kaji; project administration, Hara and Kaji; funding acquisition, Yamamoto. All authors have read and agreed to the published version of the manuscript.

Funding: This study was supported by the University's internal research funds.

Institutional Review Board Statement: Not applicable.

Informed Consent Statement: Not applicable.

Data Availability Statement: The original contributions presented in this study are included in the article material. Further inquiries can be directed to the corresponding authors.

 doi:10.20944/preprints202512.1621.v1

Conflicts of Interest: The authors declare no conflicts of interest.

Abbreviations

The following abbreviations are used in this manuscript:

Arf6	ADP-ribosylation factor 6
BCA	bicinchoninic acid
DMEM	Dulbecco's modified Eagle's medium
DSPG	Dermatan sulfate proteoglycan
FGF	fibroblast growth factor
GAG	Glycosaminoglycan
GAP	GTPase activating protein
GEF	guanine nucleotide exchange factor
HSPG	Heparan sulfate proteoglycan
MAPK	Mitogen-activated protein kinase
PG	Proteoglycan
SDS	sodium dodecyl sulfate
TGF	Transforming growth factor

References

1. Baldwin A. L., and Thurston G. Mechanics of endothelial cell architecture and vascular permeability. *Crit. Rev. Biomed. Eng.*, **2001**, *29*, 247–278. doi: 10.1615/critrevbiomedeng.v29.i2.20.
2. Maynard J. R., Dreyer B. E., Stemerman M. B., and Pitlick F. A. Tissue-factor coagulant activity of cultured human endothelial and smooth muscle cells and fibroblasts. *Blood*, **1977**, *50*, 387–396. doi: 10.1182/blood.V50.3.387.387.
3. Moncada S., Gryglewski R., Bunting S., and Vane J. R. An enzyme isolated from arteries transforms prostaglandin endoperoxides to an unstable substance that inhibits platelet aggregation. *Nature*, **1976**, *263*, 663–665. doi: 10.1038/263663a0.
4. Esmon C. T., and Owen W. G. Identification of an endothelial cell cofactor for thrombin-catalyzed activation of protein C. *Proc. Natl. Acad. Sci. USA*, **1981**, *78*, 2249–2252. doi: 10.1073/pnas.78.4.2249.
5. Levin E. G., and Loskutoff D. J. Cultured bovine endothelial cells produce both urokinase and tissue-type plasminogen activators. *J. Cell Biol.*, **1982**, *94*, 631–636. doi: 10.1083/jcb.94.3.631.
6. Van Mourik J. A., Lawrence D. A., and Loskutoff D. J. Purification of an inhibitor of plasminogen activator (antiactivator) synthesized by endothelial cells. *J. Biol. Chem.*, **1984**, *259*, 14914–14921. doi: 10.1016/S0021-9258(17)42691-3
7. Ruoslahti E. Structure and biology of proteoglycans. *Annu. Rev. Cell Biol.*, **1988**, *4*, 229–255. doi: 10.1146/annurev.cb.04.110188.001305.
8. Yamamoto C., Deng X., Fujiwara Y., and Kaji T. Proteoglycans predominantly synthesized by human brain microvascular endothelial cells in culture are perlecan and biglycan. *J. Health Sci.*, **2005**, *51*, 576–583. doi: 10.1248/jhs.51.576.
9. Saku T., and Furthmayr H. Characterization of the major heparan sulfate proteoglycan secreted by bovine aortic endothelial cells in culture. Homology to the large molecular weight molecule of basement membranes. *J. Biol. Chem.*, **1989**, *264*, 3514–3523. doi: 10.1016/S0021-9258(18)94096-2.
10. Kojima T., Shworak N. W., and Rosenberg R. D. Molecular cloning and expression of two distinct cDNA-encoding heparan sulfate proteoglycan core proteins from a rat endothelial cell line. *J. Biol. Chem.*, **1992**, *267*, 4870–4877. doi: 10.1016/S0021-9258(18)42911-0.
11. Järveläinen H. T., Kinsella M. G., Wight T. N., and Sandell L. J. Differential expression of small chondroitin/dermatan sulfate proteoglycans, PG-I/biglycan and PG-II/decorin, by vascular smooth muscle and endothelial cells in culture. *J. Biol. Chem.*, **1991**, *266*, 23274–23281. doi: 10.1016/S0021-9258(18)54493-8.
12. De Agostini A. I., Watkins S. C., Slayter H. S., Youssoufian H., and Rosenberg R. D. Localization of anticoagulantly active heparan sulfate proteoglycans in vascular endothelium: Antithrombin binding on

 doi:10.20944/preprints202512.1621.v1

cultured endothelial cells and perfused rat aorta. *J. Cell Biol.*, **1990**, *111*, 1293–1304. doi: 10.1083/jcb.111.3.1293.

13. Kojima T. Targeted gene disruption of natural anticoagulant proteins in mice. *Int. J. Hematol.*, **2002**, *76*, 36–39. doi: 10.1007/BF03165083.
14. Mertens G., Cassiman J. J., Van den Berghe H., Vermylen J., and David G. Cell surface heparan sulfate proteoglycans from human vascular endothelial cells. Core protein characterization and antithrombin III binding properties. *J. Biol. Chem.*, **1992**, *267*, 20435–20443. doi: 10.1016/S0021-9258(19)88721-5.
15. Whinna H. C., Choi H. U., Rosenberg L. C., and Church F. C. Interaction of heparin cofactor II with biglycan and decorin. *J. Biol. Chem.*, **1993**, *268*, 3920–3924. doi: 10.1016/S0021-9258(18)53560-2.
16. Kaji T., Yamada A., Miyajima S., Yamamoto C., Fujiwara Y., Wight T. N., and Kinsella M. G. Cell density-dependent regulation of proteoglycan synthesis by transforming growth factor-β1 in cultured bovine aortic endothelial cells. *J. Biol. Chem.*, **2000**, *275*, 1463–1470. doi: 10.1074/jbc.275.2.1463.
17. Hara T., Yoshida E., Fujiwara Y., Yamamoto C., and Kaji T. Transforming growth factor-β1 modulates the expression of syndecan-4 in cultured vascular endothelial cells in a biphasic manner. *J. Cell Biochem.*, **2017**, *118*, 2009–2017. doi: 10.1002/jcb.25861.
18. Kinsella M. G., Tsoi C. K., Järveläinen H. T., and Wight T. N. Selective expression and processing of biglycan during migration of bovine aortic endothelial cells. The role of endogenous basic fibroblast growth factor. *J. Biol. Chem.*, **1997**, *272*, 318–325. doi: 10.1074/jbc.272.1.318.
19. Kaji T., Yamamoto C., Oh-i M., Nishida T., and Takigawa M. Differential regulation of biglycan and decorin synthesis by connective tissue growth factor in cultured vascular endothelial cells. *Biochem. Biophys. Res. Commun.*, **2004**, *322*, 22–28. doi: 10.1016/j.bbrc.2004.07.078.
20. Kaji T., Yamamoto C., Oh-i M., Fujiwara Y., Yamazaki Y., Morita T., Plaas A. H., and Wight T. N. The vascular endothelial growth factor microvascular endothelial cells. VEGF165 induces perlecan synthesis via VEGF receptor-2 in cultured human brain. *Biochim. Biophys. Acta.*, **2006**, *1760*, 1465–1474. doi: 10.1016/j.bbagen.2006.06.010.
21. Ramasamy S., Lipke D. W., McClain C. J., and Hennig B. Tumor necrosis factor reduces proteoglycan synthesis in cultured endothelial cells. *J. Cell. Physiol.*, **1995**, *162*, 119–126. doi: 10.1002/jcp.1041620114.
22. Skop B., Sobczak A., Drózdz M., and Kotrys-Puchalska E. Comparison of the action of transforming growth factor-beta 1 and interleukin-1 beta on matrix metabolism in the culture of porcine endothelial cells. *Biochimie*, **1996**, *78*, 103–107. doi: 10.1016/0300-9084(96)82640-x.
23. Hara T., Yabushita S., Yamamoto C., and Kaji T. Cell density-dependent fibroblast growth factor-2 signaling regulates syndecan-4 expression in cultured vascular endothelial cells. *Int. J. Mol. Sci.*, **2020**, *21*, 3698. doi: 10.3390/ijms21103698.
24. Ohkawara S., Yamamoto C., Fujiwara Y., Sakamoto M., and Kaji T. Cadmium induces the production of high molecular weight heparan sulfate proteoglycan molecules in cultured vascular endothelial cells. *Environ. Toxicol. Pharmacol.*, **1997**, *3*, 187–194. doi: 10.1016/s1382-6689(97)00012-4.
25. Fujiwara Y., and Kaji T. Lead inhibits the core protein synthesis of a large heparan sulfate proteoglycan perlecan by proliferating vascular endothelial cells in culture. *Toxicology*, **1999**, *133*, 159–169. doi: 10.1016/s0300-483x(99)00027-x.
26. Hara T., Kumagai R., Tanaka T., Nakano T., Fujie T., Fujiwara Y., Yamamoto C., and Kaji T. Lead suppresses perlecan expression via EGFR-ERK1/2-COX-2-PGI2 pathway in cultured bovine vascular endothelial cells. *J. Toxicol. Sci.*, **2023**, *48*, 655–663. doi: 10.2131/jts.48.655.
27. Fujiwara Y., and Kaji T. Possible mechanism for lead inhibition of vascular endothelial cell proliferation: a lower response to basic fibroblast growth factor through inhibition of heparan sulfate synthesis. *Toxicology*, **1999**, *133*, 147–157. doi: 10.1016/S0300-483X(99)00025-6.
28. Hara T., Tatsuishi H., Banno T., Fujie T., Yamamoto C., Naka H., and Kaji T. Copper(II) bis(diethyldithiocarbamate) induces the expression of syndecan-4, a transmembrane heparan sulfate proteoglycan, via p38 MAPK activation in vascular endothelial cells. *Int. J. Mol. Sci.*, **2018**, *19*, 3302. doi: 10.3390/ijms19113302.

 doi:10.20944/preprints202512.1621.v1

29. Hara T., Kojima T., Matsuzaki H., Nakamura T., Yoshida E., Fujiwara Y., Yamamoto C., Saito S., and Kaji T. Induction of syndecan-4 by organic–inorganic hybrid molecules with a 1,10-phenanthroline structure in cultured vascular endothelial cells. *Int. J. Mol. Sci.*, **2017**, *18*, 352. doi: 10.3390/ijms18020352.
30. Hara T., Sakamaki S., Ikeda A., Nakamura T., Yamamoto C., and Kaji T. Cell density-dependent modulation of perlecan synthesis by dichloro(2,9-dimethyl-1,10-phenanthroline)zinc(II) in vascular endothelial cells. *J. Toxicol. Sci.*, **2020**, *45*, 109–115. doi: 10.2131/jts.45.109.
31. Hara T., Konishi T., Yasuike S., Fujiwara Y., Yamamoto C., and Kaji T. Sb-Phenyl-*N*-methyl-5,6,7,12-tetrahydrodibenz[*c,f*][1,5]azastibocine induces perlecan core protein synthesis in cultured vascular endothelial cells. *Int. J. Mol. Sci.*, **2023**, *24*, 3656. doi: 10.3390/ijms24043656.
32. Zhu Y., Qian H., Drake B. A., and Jin R. Atomically precise $Au_{25}(SR)_{18}$ nanoparticles as catalysts for the selective hydrogenation of α,β-unsaturated ketones and aldehydes. *Angew. Chem. Int. Ed.*, **2010**, *49*, 1295–1298. doi: 10.1002/anie.200906249.
33. Yamazoe S., Koyasu K., and Tsukuda T. Nonscalable oxidation catalysis of gold clusters. *Acc. Chem. Res.*, **2014**, *47*, 816–824. doi: 10.1021/ar400209a.
34. Knoppe S., Dolamic I., Dass A., and Bürgi T. Separation of enantiomers and CD spectra of $Au_{40}(SCH_2CH_2Ph)_{24}$: spectroscopic evidence for intrinsic chirality. *Angew. Chem. Int. Ed.*, **2012**, *51*, 7589–7591. doi: 10.1002/anie.201202369.
35. Link S., Beeby A., FitzGerald S., El-Sayed M. A., Schaaff T. G., and Whetten R. L. Visible to infrared luminescence from a 28-atom gold cluster. *J. Phys. Chem. B.*, **2002**, *106*, 3410–3415. doi: 10.1021/jp014259v.
36. Wu Z., and Jin R. On the ligand's role in the fluorescence of gold nanoclusters. *Nano Lett.*, **2010**, *10*, 2568–2573. doi: 10.1021/nl101225f.
37. Zhu M., Aikens C. M., Hendrich M. P., Gupta R., Qian H., Schatz G. C., and Jin R. Reversible switching of magnetism in thiolate-protected Au25 superatoms. *J. Am. Chem. Soc.*, **2009**, *131*, 2490–2492. doi: 10.1021/ja809157f.
38. Antonello S., Perera N. V., Ruzzi M., Gascon J. A., and Maran F. Interplay of charge state, lability, and magnetism in the molecule-like $Au_{25}(SR)_{18}$ cluster. *J. Am. Chem. Soc.*, **2013**, *135*, 15585–15594. doi: 10.1021/ja407887d.
39. Yamazoe S., Takano S., Kurashige W., Yokoyama T., Nitta K., Negishi Y., and Tsukuda T. Hierarchy of bond stiffnesses within icosahedral-based gold clusters protected by thiolates. *Nat. Commun.*, **2016**, *7*, 10414. doi: 10.1038/ncomms10414.
40. Negishi Y., Sakamoto C., Ohyama T., and Tsukuda T. Synthesis and the origin of the stability of thiolate-protected Au_{130} and Au_{187} clusters. *J. Phys. Chem. Lett.*, **2012**, *3*, 1624–1628. doi: 10.1021/jz300547d.
41. Ohta T., Shibuta M., Tsunoyama H., Negishi Y., Eguchi T., and Nakajima A. Size and structure dependence of electronic states in thiolate-protected gold nanoclusters of $Au_{25}(SR)_{18}$, $Au_{38}(SR)_{24}$, and $Au_{144}(SR)_{60}$. *J. Phys. Chem. C.*, **2013**, *117*, 3674–3679. doi: 10.1021/jp400785f.
42. Negishi Y., Nobusada K., and Tsukuda T. Glutathione-protected gold clusters revisited: bridging the gap between gold(I)–thiolate complexes and thiolate-protected gold nanocrystals. *J. Am. Chem. Soc.*, **2005**, *127*, 5261–5270. doi: 10.1021/ja042218h.
43. Wu Z., Gayathri C., Gil R. R., and Jin R. Probing the structure and charge state of glutathione-capped $Au_{25}(SG)_{18}$ clusters by NMR and mass spectrometry. *J. Am. Chem. Soc.*, **2009**, *131*, 6535–6542. doi: 10.1021/ja900386s.
44. Shichibu Y., Negishi Y., Tsukuda T., and Teranishi T. Large-scale synthesis of thiolated Au25 clusters via ligand exchange reactions of phosphine-stabilized Au11 clusters. *J. Am. Chem. Soc.*, **2005**, *127*, 13464–13465. doi: 10.1021/ja053915s.
45. Hara T., Sakuma M., Fujie T., Kaji T., and Yamamoto C. Cadmium induces plasminogen activator inhibitor-1 via Smad2/3 signaling pathway in human endothelial EA.hy926 cells. *J. Toxicol. Sci.*, **2021**, *46*, 249–253. doi: 10.2131/jts.46.249.
46. Hara T., Saeki M., Negishi Y., Kaji T., and Yamamoto C. Cell density-dependent accumulation of low polarity gold nanocluster in cultured vascular endothelial cells. *J. Toxicol. Sci.*, **2020**, *45*, 795–800. doi: 10.2131/jts.45.795.

47. Wennerberg K., Rossman K. L., and Der C. J. The Ras superfamily at a glance. *J. Cell Sci.*, **2005**, *118*, 843–846. doi: 10.1242/jcs.01660.
48. Miura K., Nam J. M., Kojima C., Mochizuki N., and Sabe H. EphA2 engages Git1 to suppress Arf6 activity modulating epithelial cell–cell contacts. *Mol. Biol. Cell.*, **2009**, *20*, 1949–1959. doi: 10.1091/mbc.e08-06-0549.
49. Goldberg R. L., Parrott D. P., Kaplan S. R., and Fuller G. C. A mechanism of action of gold sodium thiomalate in diseases characterized by a proliferative synovitis: reversible changes in collagen production in cultured human synovial cells. *J. Pharmacol. Exp. Ther.*, **1981**, *218*, 395–403. doi: 10.1016/S0022-3565(25)32683-2.
50. Finkelstein A. E., Walz D. T., Batista V., Mizraji M., Roisman F., and Misher A. A. Auranofin. New oral gold compound for treatment of rheumatoid arthritis. *Ann. Rheum. Dis.*, **1976**, *35*, 251. doi: 10.1136/ard.35.3.251.
51. Storhoff J. J., and Mirkin C. A. Programmed materials synthesis with DNA. *Chem. Rev.*, **1999**, *99*, 1849–1862. doi: 10.1021/cr970071p.
52. Voskerician G., Shive M. S., Shawgo R. S., von Recum H., Anderson J. M., Cima M. J., and Langer R. Biocompatibility and biofouling of MEMS drug delivery devices. *Biomaterials*, **2003**, *24*, 1959–1967. doi: 10.1016/S0142-9612(02)00565-3.
53. Shang L., Stockmar F., Azadfar N., and Nienhaus G. U. Intracellular thermometry by using fluorescent gold nanoclusters. *Angew. Chem. Int. Ed.*, **2013**, *52*, 11154–11157. doi: 10.1002/anie.201306366.
54. Chen L. Y., Wang C. W., Yuan Z. Q., and Chang H. T. Fluorescent gold nanoclusters: recent advances in sensing and imaging. *Anal. Chem.*, **2015**, *87*, 216–229. doi: 10.1021/ac503636j.
55. Zhang X. D., Luo Z., Chen J., Shen X., Song S., Sun Y., Fan S., Fan F., Leong D. T., and Xie J. Ultrasmall $Au_{10-12}(SG)_{10-12}$ nanomolecules for high tumor specificity and cancer radiotherapy. *Adv. Mater.*, **2014**, *26*, 4565–4568. doi: 10.1002/adma.201400866.
56. Riley R. S., and Day E. S. Gold nanoparticle-mediated photothermal therapy: applications and opportunities for multimodal cancer treatment. *Wiley Interdiscip. Rev. Nanomed. Nanobiotechnol.*, **2017**, *9*. doi: 10.1002/wnan.1449.
57. Perrault S. D., Walkey C., Jennings T., Fischer H. C., and Chan W. C. Mediating tumor targeting efficiency of nanoparticles through design. *Nano Lett.*, **2009**, *9*, 1909–1915. doi: 10.1021/nl900031y.
58. Chou L. Y., and Chan W. C. Fluorescence-tagged gold nanoparticles for rapidly characterizing the size-dependent biodistribution in tumor models. *Adv. Healthc. Mater.*, **2012**, *1*, 714–721. doi: 10.1002/adhm.201200084.
59. Zhang X. D., Wu D., Shen X., Chen J., Sun Y. M., Liu P. X., and Liang X. J. Size-dependent radiosensitization of PEG-coated gold nanoparticles for cancer radiation therapy. *Biomaterials*, **2012**, *33*, 6408–6419. doi: 10.1016/j.biomaterials.2012.05.047.
60. Goodman C. M., McCusker C. D., Yilmaz T., and Rotello V. M. Toxicity of gold nanoparticles functionalized with cationic and anionic side chains. *Bioconjug. Chem.*, **2004**, *15*, 897–900. doi: 10.1021/bc049951i.
61. Hoffmann F., Cinatl J., Kabičková H., Kreuter J., and Stieneker F. Preparation, characterization and cytotoxicity of methylmethacrylate copolymer nanoparticles with a permanent positive surface charge. *Int. J. Pharm.*, **1997**, *157*, 189–198. doi: 10.1016/S0378-5173(97)00242-1.
62. Jiang Y., Huo S., Mizuhara T., Das R., Lee Y. W., Hou S., Moyano D. F., Duncan B., Liang X. J., and Rotello V. M. The interplay of size and surface functionality on the cellular uptake of sub-10 nm gold nanoparticles. *ACS Nano.*, **2015**, *9*, 9986–9993. doi: 10.1021/acsnano.5b03521.
63. Foroozandeh P., and Aziz A. A. Insight into cellular uptake and intracellular trafficking of nanoparticles. *Nanoscale Res. Lett.*, **2018**, *13*, 339. doi: 10.1186/s11671-018-2728-6.
64. Yang L., Shang L., and Nienhaus G. U. Mechanistic aspects of fluorescent gold nanocluster internalization by live HeLa cells. *Nanoscale*, **2013**, *5*, 1537–1543. doi: 10.1039/C2NR33147K.
65. Barbieri E., Di Fiore P. P., and Sigismund S. Endocytic control of signaling at the plasma membrane. *Curr. Opin. Cell Biol.*, **2016**, *39*, 21–27. doi: 10.1016/j.ceb.2016.01.012.
66. Takei K., and Haucke V. Clathrin-mediated endocytosis: membrane factors pull the trigger. *Trends Cell Biol.*, **2001**, *11*, 385–391. doi: 10.1016/s0962-8924(01)02082-7.
67. Harris J., Werling D., Hope J. C., Taylor G., and Howard C. J. Caveolae and caveolin in immune cells: distribution and functions. *Trends Immunol.*, **2002**, *23*, 158–164. doi: 10.1016/s1471-4906(01)02161-5.

 doi:10.20944/preprints202512.1621.v1

68. Lamaze C., and Schmid S. L. The emergence of clathrin-independent pinocytic pathways. *Curr. Opin. Cell Biol.*, **1995**, *7*, 573–580. doi: 10.1016/0955-0674(95)80015-8.
69. Boucrot E., and Kirchhausen T. Endosomal recycling controls plasma membrane area during mitosis. *Proc. Natl. Acad. Sci. USA.*, **2007**, *104*, 7939–7944. doi: 10.1073/pnas.0702511104.
70. Lisanti M. P., Scherer P. E., Vidugiriene J., Tang Z., Hermanowski-Vosatka A., Tu Y. H., Cook R. F., and Sargiacomo M. Characterization of caveolin-rich membrane domains isolated from an endothelial-rich source: implications for human disease. *J. Cell Biol.*, **1994**, *126*, 111–126. doi: 10.1083/jcb.126.1.111.
71. Boucrot E., Howes M. T., Kirchhausen T., and Parton R. G. Redistribution of caveolae during mitosis. *J. Cell Sci.*, **2011**, *124*, 1965–1972. doi: 10.1242/jcs.076570.
72. Hinze C., and Boucrot E. Endocytosis in proliferating, quiescent and terminally differentiated cells. *J. Cell Sci.*, **2018**, *131*, jcs216804. doi: 10.1242/jcs.216804.
73. Béglé A., Tryoen-Tóth P., de Barry J., Bader M. F., and Vitale N. ARF6 regulates the synthesis of fusogenic lipids for calcium-regulated exocytosis in neuroendocrine cells. *J. Biol. Chem.*, **2009**, *284*, 4836–4845. doi: 10.1074/jbc.M806894200.
74. Zimmermann P., Zhang Z., Degeest G., Mortier E., Leenaerts I., Coomans C., Schulz J., N'Kuli F., Courtoy P. J., and David G. Syndecan recycling is controlled by syntenin-PIP_2 interaction and Arf6. *Dev. Cell.*, **2005**, *9*, 377–388. doi: 10.1016/j.devcel.2005.07.011.
75. Renault L., Guibert B., and Cherfils J. Structural snapshots of the mechanism and inhibition of a guanine nucleotide exchange factor. *Nature*, **2003**, *426*, 525–530. doi: 10.1038/nature02197.
76. Gaschet J., and Hsu V. W. Distribution of ARF6 between membrane and cytosol is regulated by its GTPase cycle. *J. Biol. Chem.*, **1999**, *274*, 20040–20045. doi: 10.1074/jbc.274.28.20040.
77. Donaldson J. G., and Jackson C. L. ARF family G proteins and their regulators: roles in membrane transport, development and disease. *Nat. Rev. Mol. Cell Biol.*, **2011**, *12*, 362–375. doi: 10.1038/nrm3117.
78. Hongu T., and Kanaho Y. Activation machinery of the small GTPase Arf6. *Adv. Biol. Regul.*, **2014**, *54*, 59–66. doi: 10.1016/j.jbior.2013.09.014.
79. Aviezer D., Hecht D., Safran M., Eisinger M., David G., and Yayon A. Perlecan, basal lamina proteoglycan, promotes basic fibroblast growth factor-receptor binding, mitogenesis, and angiogenesis. *Cell.*, **1994**, *79*, 1005–1013. doi: 10.1016/0092-8674(94)90031-0
80. Santy L. C., and Casanova J. E. Activation of ARF6 by ARNO stimulates epithelial cell migration through downstream activation of both Rac1 and phospholipase D. *J. Cell Biol.*, **2001**, *154*, 599–610. doi: 10.1083/jcb.200104019.
81. Knizhnik A. V., Kovaleva O. V., Komelkov A. V., Trukhanova L. S., Rybko V. A., Zborovskaya I. B., and Tchevkina E. M. Arf6 promotes cell proliferation via the PLD-mTORC1 and p38MAPK pathways. *J. Cell. Biochem.*, **2012**, *113*, 360–371. doi: 10.1002/jcb.23362.